where $h : [0, \infty) \to R$ is a bounded function. Note that $\sigma_F(\cdot)[h]$ is the Fisher information (Murphy 1995, p. 189) with h being the index of infinite-dimensional parameters. Appendix B1 shows that $\sqrt{n}(\hat{F}(t) - F(t))$ converges weakly to a Gaussian process $G_F(t)$ with $E[G_F(t)] = 0$ and

$$E[G_F(s)G_F(t)] = \int w_s(x)\sigma_F^{-1}(w_t)(x)dF(x),$$

where $w_s(x) \equiv \mathbf{I}(x \le s)$ and $\sigma_F^{-1}(w_t)$ solves $\sigma_F(x)[h] = w_t(x)$ for h.

Consider the empirical estimator of $\sigma_F(x)[h]$ as

$$\hat{\sigma}_F(x)[h] = \frac{1}{n}\sum_{i=1}^{n} \mathbf{I}(U_i \le x \le V_i)\left\{\frac{1}{\hat{F}_i}h(x) - \frac{1}{\hat{F}_i^2}\sum_{k=1}^{n} J_{ik}h_k\hat{f}_k\right\},$$

where $h_k = h(T_k)$. Then, the plug-in covariance estimator is

$$\hat{E}[G_F(s)G_F(t)] = \int w_s(x)\hat{\sigma}_F^{-1}(w_t)(x)d\hat{F}(x) = \sum_{j=1}^{n} w_s(T_j)\hat{\sigma}_F^{-1}(w_t)(T_j)\hat{f}_j.$$

After some matrix calculations given in Appendix B2, one can verify

$$\sum_{j=1}^{n} w_s(T_j)\hat{\sigma}_F^{-1}(w_t)(T_j)\hat{f}_j = \mathbf{W}_s^{\mathrm{T}}\left\{\frac{i_n(\hat{\mathbf{f}})}{n}\right\}^{-1}\mathbf{W}_t,$$

where $\mathbf{W}_t = (\mathbf{I}(T_{(1)} \le t) - \mathbf{I}(T_{(n)} \le t), \ldots, \mathbf{I}(T_{(n-1)} \le t) - \mathbf{I}(T_{(n)} \le t))^{\mathrm{T}}$ and $i_n(\mathbf{f})$ is given in Eq. (2). Therefore, we obtain a plug-in covariance estimator

$$\hat{C}ov\{\hat{F}(s), \hat{F}(t)\} = \mathbf{W}_s^{\mathrm{T}}\left[D\left\{\mathrm{diag}\left(\frac{1}{\hat{\mathbf{f}}^2}\right) - J^{\mathrm{T}}\mathrm{diag}\left(\frac{1}{\hat{\mathbf{F}}^2}\right)J\right\}D^{\mathrm{T}}\right]^{-1}\mathbf{W}_t, \quad (3)$$

and a variance estimator

$$\hat{V}_{\mathrm{Info}}\{\hat{F}(t)\} = \mathbf{W}_t^{\mathrm{T}}\left[D\left\{\mathrm{diag}\left(\frac{1}{\hat{\mathbf{f}}^2}\right) - J^{\mathrm{T}}\mathrm{diag}\left(\frac{1}{\hat{\mathbf{F}}^2}\right)J\right\}D^{\mathrm{T}}\right]^{-1}\mathbf{W}_t. \quad (4)$$

Remark: Murphy (1995), Zeng and Lin (2006), Chen (2010), and Emura and Wang (2012) use similar techniques to derive variance estimators. However, none of them results in an explicit form like Eqs. (3) and (4).

4 Inference based on the asymptotic covariance estimator

This section examines various inference procedures based on the proposed covariance estimator.

4.1 Pointwise confidence interval

Applying the variance estimator $\hat{V}_{\text{Info}}\{\hat{F}(t)\}$ in Eq. (4) and the asymptotic normality, we propose a pointwise confidence interval. Log-transformation and arcsine-square root transformation are known to improve the coverage performance over the linear confidence interval (Klein and Moeschberger 2003, pp. 104–108). Here, we apply the log-transformed interval based on $\log \hat{F}(t) - \log F(t) \sim N(\,0,\ \hat{V}_{\text{Info}}\{\,\hat{F}(t)\,\}/\hat{F}(t)^2)$. Hence, the $(1-\alpha)100\%$ confidence interval for $F(t)$ is

$$(\ \hat{F}(t)\exp[\ -z_{\alpha/2}\hat{V}_{\text{Info}}^{1/2}\{\hat{F}(t)\}/\hat{F}(t)\ ],\quad \hat{F}(t)\exp[\ z_{\alpha/2}\hat{V}_{\text{Info}}^{1/2}\{\hat{F}(t)\}/\hat{F}(t)\ ]\ ),$$

where $z_{\alpha/2}$ is the $(1-\alpha/2)100\%$ point of the standard normal distribution.

4.2 Goodness-of-fit test

We consider a goodness-of-fit test for

$$H_0:\ \ F = F_0 \text{ vs. } H_1:\ \ F \neq F_0,$$

where F_0 is a known continuous distribution function. Applying the continuous mapping theorem to the results of Sect. 3.2, we have

$$\sqrt{n}\sup_t|\ \hat{F}(t) - F(t)| \xrightarrow{d} \sup_t |G_F(t)|.$$

The asymptotic distribution can be easily simulated after estimating the covariance structure of $G_{F_0}(t)$ with Eq. (3). Ideally, the asymptotic distribution is approximated by that of $\max_j |G_{F_0}(t_j)|$ for fixed fine grids $t_j : j = 1,\ \ldots,\ N$ with large N. Here, we suggest a practically convenient choice of $t_j = T_{(j)}$, $j = 1,\ \ldots,\ n-1$, which leads to a simple algorithm and achieves good finite sample performance. The algorithm is stated as follows:

Kolmogorov–Smirnov test for $H_0:\ \ F = F_0$ vs. $H_1:\ \ F \neq F_0$;

Step 1: Calculate $K = \sup_t|\ \hat{F}(t) - F_0(t)|$ and $i_n(\hat{\mathbf{f}})$.

Step 2: Generate $\mathbf{G}^{(b)} = (G_1^{(b)}, \ldots, G_{n-1}^{(b)}) \sim N(\mathbf{0}_{n-1}, Hi_n(\hat{\mathbf{f}})^{-1}H^{\mathrm{T}})$ for $b = 1, \ldots, B$, and compute $K^{(b)} = \max_{i=1,\ldots,n-1}|G_i^{(b)}|$, where $H = (\ \mathbf{W}_{T_{(1)}}, \ldots, \mathbf{W}_{T_{(n-1)}})^{\mathrm{T}}$.

Step 3: Reject $H_0:\ F = F_0$ with level α if $\sum_{b=1}^{B}\mathbb{I}(\ K^{(b)} > K\ )/B < \alpha$.

Similarly, we can test $H_0:\ \ F = F_0$ using the Cramér–von Mises statistic

$$C = n\int_0^\infty \{\ \hat{F}(t) - F_0(t)\ \}^2 dF_n(t) = \sum_{j=1}^{n}\{\ \hat{F}(T_j) - F_0(T_j)\ \}^2,$$

where $F_n(t) = \sum_{j=1}^{n}\mathbb{I}(T_j \le t)/n$ is the empirical distribution function.

Cramér–von Mises test for $H_0: \ F = F_0$ vs. $H_1: \ F \neq F_0$;

Step 1: Calculate $C = \sum_{j=1}^{n} \{ \hat{F}(T_j) - F_0(T_j) \}^2$ and $i_n(\hat{\mathbf{f}})$.
Step 2: Generate $\mathbf{G}^{(b)} = (G_1^{(b)}, \ \ldots, \ G_{n-1}^{(b)}) \sim N(\mathbf{0}_{n-1}, \ H i_n(\hat{\mathbf{f}})^{-1} H^{\mathrm{T}})$ for $b = 1, \ \ldots, \ B$, and then compute $C^{(b)} = (\mathbf{G}^{(b)})^{\mathrm{T}} \mathbf{G}^{(b)}$.
Step 3: Reject $H_0: \ F = F_0$ with level α if $\sum_{b=1}^{B} \mathbf{I}(\ C^{(b)} > C \ )/B < \alpha$.

4.3 Confidence band

The confidence band covers the true function $F(t)$ at all t for a specified confidence level $(1 - \alpha)$. We follow the construction of two most well-known confidence bands for the survival function under right-censoring, namely, the equal precision (EP) band and Hall–Wellner (HW) band (Nair 1984; Klein and Moeschberger 2003, Sect. 4.4).

Let $\psi(u)$ be a nonnegative continuous function. Applying the continuous mapping theorem to the results of Sect. 3.2, we have

$$\sqrt{n} \sup_t | \ \psi\{ \ F(t) \ \}\{ \ \hat{F}(t) - F(t) \ \}| \xrightarrow{d} \sup_t |\psi\{ \ F(t) \ \} G_F(t)|.$$

Then, the confidence bands are obtained by solving

$$1 - \alpha = \Pr\left\{ \sup_t | \ \psi\{ \ F(t) \ \}\{ \ \hat{F}(t) - F(t) \ \}| \ \leq c_{1-\alpha}(\psi) \right\},$$

where $c_{1-\alpha}(\psi)$ is the $(1 - \alpha)100\%$ point of $\sup_t |\psi\{ \ F(t) \ \} G_F(t)/\sqrt{n}|$.

The EP band corresponds to $\psi(u) = \{ \ u(\ 1 - u \ ) \ \}^{-1/2}$. In practice, it is desirable to make $\psi(u)$ bounded. Following Nair (1984), we alternatively use $\psi_{EP}(u) = \{ \ (\ u \vee p_1 \ )(\ 1 - u \wedge p_2 \ ) \ \}^{-1/2}$, $0 < p_1 < p_2 < 1$, to yield the EP band

$$\hat{F}(t) \pm c_{1-\alpha}(\psi_{EP}) \sqrt{\{ \ \hat{F}(t) \vee p_1 \ \}\{ \ 1 - \hat{F}(t) \wedge p_2 \ \}}.$$

We set p_1 =0.1 or 0.2 and p_2 =0.8 or 0.9 as suggested by Nair (1984).

The HW band corresponds to $\psi_{HW}(u) \equiv 1$, which is the version of Kolmogorov–Smirnov band for uncensored data. The HW band is

$$\hat{F}(t) \pm c_{1-\alpha}(\psi_{HW}),$$

where $c_{1-\alpha}(\psi_{HW})$ is obtained as the $(1 - \alpha)100\%$ point for $\{ \ K^{(b)}; \ b = 1, \ \ldots, \ B \ \}$ in Step 2 of the Kolmogorov–Smirnov test.

The bootstrap is useful to validate the coverage performance of the confidence bands above. First, the bootstrap NPMLEs, denoted as $\{ \ \hat{F}_b^*, \ b = 1, \ \ldots, \ B \ \}$, are computed (see Step 1 of Appendix A). Then, approximately $(1 - \alpha)100\%$ of the bootstrap NPMLEs should fall inside the band. This validation scheme will be illustrated with real data analysis.

5 Simulations

Extensive simulations have been conducted to investigate the performances of the proposed methods and to compare them with the bootstrap and jackknife methods.

We adopt the same design used in Moreira and Uña-Álvarez (2010). They consider models $U^* \sim \text{Unif}(0,\ a)$, $T^* \sim \text{Unif}(0,\ 1)$, and $V^* \sim \text{Unif}(b,\ 1)$, where $(a,\ b) = (0.25,\ 0.75)$, $(0.5,\ 0.5)$ or $(0.67,\ 0.33)$. The corresponding sample inclusion probabilities are $\Pr(U^* \leq T^* \leq V^*) = (1 - a + b)/2$ =0.75, 0.5 and 0.33, respectively. They also consider a model $U^* \sim \text{Unif}(-5,\ 15)$, $T^* \sim \text{Unif}(0,\ 15)$, and $V^* = U^* + c$, where c =5. This model is important since it yields a situation similar to the childhood cancer example.

Based on simulated samples, we compute the relevant quantities (NPMLE, confidence interval, goodness-of-fit statistic, and confidence band) for 500 repetitions. We choose $B = 1000$ for the number of resamplings.

5.1 Performance of the covariance estimator

For r $(= 1,\ \ldots,\ 500)$-th repetition, we compute the NPMLE $\hat{F}(s)_{(r)}$, $\hat{F}(t)_{(r)}$ and the covariance estimator $\hat{C}ov\{\ \hat{F}(s),\ \hat{F}(t)\ \}_{(r)}$ in Eq. (3). We compare the average of the estimated covariance

$$\frac{1}{500}\sum_{r=1}^{500} \hat{C}ov\left\{\ \hat{F}(s),\ \hat{F}(t)\ \right\}_{(r)}$$

with the sample covariance

$$\frac{1}{500}\sum_{r=1}^{500}\left\{\ \hat{F}(s)_{(r)} - \bar{\hat{F}}(s)\right\}\left\{\ \hat{F}(t)_{(r)} - \bar{\hat{F}}(t)\right\}.$$

where $\bar{\hat{F}}(s) = \sum_{r=1}^{500} \hat{F}(s)_{(r)}/500$. As shown in Table 1, the differences between the estimated covariance and the sample covariance are very small for all configurations. The sample covariance between $\hat{F}(s)_{(r)}$ and $\hat{F}(t)_{(r)}$ increases as the distance $|t - s|$ decreases, which is a similar behavior to that of the empirical distribution function from un-truncated data.

5.2 Comparison with the bootstrap and jackknife methods

We compare the performance of the proposed variance estimator ($\hat{V}_{\text{Info}}\{\hat{F}(t)\}$), the bootstrap estimator ($\hat{V}_{\text{Boot}}\{\hat{F}(t)\}$) and the jackknife estimator ($\hat{V}_{\text{Jack}}\{\hat{F}(t)\}$) for fixed t. We compute the average of the estimated standard deviation (SD)

$$\frac{1}{500}\sum_{r=1}^{500}\sqrt{\hat{V}\{\hat{F}(t)\}_{(r)}}$$

Table 1 Simulation results of the proposed covariance estimator based on 500 replications

		$n = 100$		$n = 250$	
	$(s,\ t)$	Sample covariance	Estimated covariance	Sample covariance	Estimated covariance
$a = 0.25, b = 0.75$	(0.2, 0.5)	0.00565	0.00595	0.00195	0.00180
	(0.4, 0.5)	0.00655	0.00668	0.00234	0.00215
	(0.2, 0.8)	0.00279	0.00366	0.00112	0.00110
$a = 0.5, b = 0.5$	(0.2, 0.5)	0.00641	0.00704	0.00266	0.00258
	(0.4, 0.5)	0.00833	0.00877	0.00335	0.00336
	(0.2, 0.8)	0.00378	0.00450	0.00184	0.00169
$a = 0.067, b = 0.33$	(0.2, 0.5)	0.00366	0.00374	0.00157	0.00141
	(0.4, 0.5)	0.00677	0.00645	0.00283	0.00245
	(0.2, 0.8)	0.00356	0.00350	0.00159	0.00130
$c = 5$	(3.0, 7.5)	0.01166	0.01291	0.00525	0.00511
	(6.0, 7.5)	0.02027	0.02068	0.00860	0.00845
	(3.0, 12.0)	0.00558	0.00654	0.00269	0.00260

Data are generated from $U^* \sim \text{Unif}(0,\ a)$, $T^* \sim \text{Unif}(0,\ 1)$, and $V^* \sim \text{Unif}(b,\ 1)$ in the first three cases, and from $U^* \sim \text{Unif}(-5,\ 15)$, $T^* \sim \text{Unif}(0,\ 15)$, and $V^* = U^* + c$ in the last case

Sample covariance = $\frac{1}{500}\sum_{r=1}^{500}\{\hat{F}(s)_{(r)} - \bar{\hat{F}}(s)_{(r)}\}\{\hat{F}(t)_{(r)} - \bar{\hat{F}}(t)_{(r)}\}$

Estimated covariance = $\frac{1}{500}\sum_{r=1}^{500}\hat{Cov}\{\hat{F}(s),\ \hat{F}(t)\}_{(r)}$

where $\hat{V}\{\hat{F}(t)\}_{(r)}$ is a variance estimator for the rth repetition, and compare it with $\text{SD}\{\hat{F}(t)\}$, the sample standard deviation (SD) for $\hat{F}(t)_{(r)}$, $r = 1, \ldots, 500$. The performance of the three methods are measured with the mean squared error

$$\text{MSE} = \frac{1}{500}\sum_{r=1}^{500}\left(\sqrt{\hat{V}\{\hat{F}(t)\}_{(r)}} - \text{SD}\{\hat{F}(t)\}\right)^2.$$

We also compare the performance of the three methods in terms of the coverage performance of the 95% confidence interval.

Tables 2 and 3 show the results under the models $U^* \sim \text{Unif}(0,\ a)$, $T^* \sim \text{Unif}(0,\ 1)$, and $V^* \sim \text{Unif}(b,\ 1)$, where $(a,\ b) = (0.25,\ 0.75)$ and $(0.5,\ 0.5)$, respectively. All the three variance estimators correctly capture the estimates of $\text{SD}\{\hat{F}(t)\}$. Among the three estimators, the jackknife has the smallest bias. In terms of MSE, the bootstrap is the best for small samples, while the proposed method tends to be the best for large samples. For instance, the bootstrap is the best for $n = 100$, while the proposed method is the best for n =200, 250 and 300 (Table 2). The jackknife has the largest MSE in most configurations.

All the three methods generally produce the nominal 95% coverage performance at $t = 0.5$ ($F(t) = 0.5$). However, at the tail $t = 0.2$ ($F(t) = 0.2$), the bootstrap method often results in serious under-coverage. The magnitude of the under-coverage of the bootstrap is similar to that reported in the simulation results of Moreira and Uña-Álvarez (2010). Both the proposed and the jackknife methods alleviate the under-

Table 2 Simulation results under $U^* \sim$ Unif(0, a), $T^* \sim$ Unif(0, 1), and $V^* \sim$ Unif(b, 1) with a= 0.25 and b = 0.75 based on 500 replications

		n = 100	n = 150	n = 200	n = 250	n = 300
$F(t) = 0.5$						
SD		0.083	0.064	0.053	0.050	0.046
ESD	Proposed	0.070	0.057	0.050	0.045	0.042
	Bootstrap	0.070	0.059	0.051	0.046	0.043
	Jackknife	0.075	0.061	0.053	0.047	0.044
MSE	Proposed	0.00219	0.00086	0.00033	0.00028	0.00026
	Bootstrap	0.00104	0.00070	0.00048	0.00038	0.00035
	Jackknife	0.00296	0.00185	0.00094	0.00075	0.00073
95%Cov	Proposed	0.930	0.942	0.950	0.946	0.938
	Bootstrap	0.920	0.938	0.950	0.942	0.948
	Jackknife	0.930	0.950	0.948	0.946	0.940
$F(t) = 0.2$						
SD		0.090	0.065	0.057	0.052	0.048
ESD	Proposed	0.069	0.056	0.049	0.045	0.041
	Bootstrap	0.069	0.058	0.051	0.046	0.042
	Jackknife	0.074	0.061	0.053	0.047	0.043
MSE	Proposed	0.00394	0.00091	0.00073	0.00052	0.00044
	Bootstrap	0.00213	0.00113	0.00094	0.00067	0.00055
	Jackknife	0.00522	0.00248	0.00189	0.00115	0.00103
95%Cov	Proposed	0.938	0.942	0.946	0.932	0.942
	Bootstrap	0.898	0.910	0.928	0.908	0.924
	Jackknife	0.940	0.948	0.952	0.938	0.950

ESD = $\frac{1}{500}\sum_{r=1}^{500}\sqrt{\hat{V}\{\hat{F}(t)\}_{(r)}}$

MSE = $\frac{1}{500}\sum_{r=1}^{500}\left(\sqrt{\hat{V}\{\hat{F}(t)\}_{(r)}} - \mathrm{SD}\{\hat{F}(t)\}\right)^2$

95%Cov = Empirical coverage probability of the 95% confidence interval

coverage at the tail. Interestingly, the jackknife is quite competitive with the proposed method in terms of coverage performance despite the poor performance of the MSE.

Table 4 shows the results under the model $U^* \sim$ Unif(−5, 15), $T^* \sim$ Unif(0, 15), and $V^* = U^* + 5$. All the three variance estimators are nearly unbiased and their MSEs are very similar. Although the bootstrap seems to provide the best result in terms of the MSE, the three methods are quite competitive. In terms of coverage probability, the bootstrap tends to be the best.

Although we found no single best method across all criteria, the advantage of the proposed method over other methods appears for larger samples (n = 250 and 300). The MSE of the proposed method is smallest in majority of cases. Unlike the bootstrap that may exhibit serious under-coverage at the tails, the proposed method can alleviate the problem for large sample sizes. As for the computational cost among the three methods, the proposed method is the lowest since it merely performs the matrix algebra in Eq. (4). On the other extreme, the bootstrap requires performing the

Table 3 Simulation results under $U^* \sim \text{Unif}(0,\ a)$, $T^* \sim \text{Unif}(0,\ 1)$, and $V^* \sim \text{Unif}(b,\ 1)$ with $a = 0.5$ and $b = 0.5$ based on 500 replications

		$n = 100$	$n = 150$	$n = 200$	$n = 250$	$n = 300$
$F(t) = 0.5$						
SD		0.093	0.078	0.068	0.059	0.055
ESD	Proposed	0.084	0.070	0.060	0.054	0.049
	Bootstrap	0.086	0.071	0.061	0.055	0.050
	Jackknife	0.092	0.076	0.063	0.057	0.051
MSE	Proposed	0.00237	0.00227	0.00141	0.00069	0.00059
	Bootstrap	0.00125	0.00104	0.00061	0.00054	0.00040
	Jackknife	0.00385	0.00326	0.00161	0.00150	0.00087
95%Cov	Proposed	0.932	0.934	0.950	0.952	0.958
	Bootstrap	0.934	0.944	0.954	0.952	0.958
	Jackknife	0.934	0.944	0.950	0.964	0.962
$F(t) = 0.2$						
SD		0.093	0.074	0.065	0.059	0.052
ESD	Proposed	0.080	0.066	0.058	0.052	0.048
	Bootstrap	0.084	0.069	0.060	0.054	0.049
	Jackknife	0.090	0.073	0.061	0.055	0.050
MSE	Proposed	0.00270	0.00132	0.00077	0.00055	0.00035
	Bootstrap	0.00237	0.00152	0.00087	0.00071	0.00046
	Jackknife	0.00551	0.00366	0.00138	0.00119	0.00051
95%Cov	Proposed	0.932	0.938	0.946	0.928	0.926
	Bootstrap	0.908	0.902	0.934	0.924	0.910
	Jackknife	0.944	0.950	0.952	0.942	0.938

$\text{ESD} = \frac{1}{500}\sum_{r=1}^{500}\sqrt{\hat{V}\{\hat{F}(t)\}_{(r)}}$

$\text{MSE} = \frac{1}{500}\sum_{r=1}^{500}\left(\sqrt{\hat{V}\{\hat{F}(t)\}_{(r)}} - \text{SD}\{\hat{F}(t)\}\right)^2$

95%Cov = Empirical coverage probability of the 95% confidence interval

self-consistency algorithms over $B = 1{,}000$ resamplings. Hence, the proposed method would be useful when the sample size is large.

5.3 Performance of the goodness-of-fit test

First, we examine the type I error of the goodness-of-fit tests introduced in Sect. 4.2. For each run, we record the rejection/acceptance status of the goodness-of-fit tests at the $100\alpha\%$ level, and calculate the rejection rates among 500 repetitions. We also compare the null means of the tests (denoted by $E[C]$ and $E[K]$) with the resampling means (denoted by $E[C^{(b)}]$ and $E[K^{(b)}]$).

As shown in Table 5, the rejection rates (type I error rates) are in good agreement with the selected nominal sizes ($\alpha = 0.01, 0.05$, and 0.10). In addition, the sample means $E[C]$ and $E[K]$ are close to the resampling means $E[C^{(b)}]$ and $E[K^{(b)}]$, respectively.

Table 4 Simulation results under $U^* \sim$ Unif(−5, 15), $T^* \sim$ Unif(0, 15), and $V^* = U^* + 5$ based on 500 replications

		$n = 100$	$n = 150$	$n = 200$	$n = 250$	$n = 300$
$F(t) = 0.5$						
SD		0.146	0.121	0.103	0.096	0.086
ESD	Proposed	0.146	0.120	0.105	0.094	0.086
	Bootstrap	0.147	0.120	0.105	0.094	0.086
	Jackknife	0.156	0.125	0.108	0.096	0.088
MSE	Proposed	0.00064	0.00023	0.00013	0.000065	0.000046
	Bootstrap	0.00048	0.00020	0.00010	0.000069	0.000046
	Jackknife	0.00089	0.00026	0.00014	0.000067	0.000047
95%Cov	Proposed	0.904	0.932	0.946	0.928	0.928
	Bootstrap	0.940	0.944	0.950	0.950	0.930
	Jackknife	0.910	0.936	0.946	0.940	0.936
$F(t) = 0.2$						
SD		0.101	0.084	0.071	0.064	0.057
ESD	Proposed	0.100	0.081	0.070	0.062	0.057
	Bootstrap	0.106	0.083	0.072	0.063	0.058
	Jackknife	0.107	0.084	0.072	0.064	0.058
MSE	Proposed	0.00109	0.00048	0.00027	0.00018	0.00012
	Bootstrap	0.00097	0.00044	0.00024	0.00017	0.00012
	Jackknife	0.00133	0.00053	0.00028	0.00018	0.00013
95%Cov	Proposed	0.938	0.944	0.946	0.942	0.948
	Bootstrap	0.958	0.946	0.954	0.944	0.948
	Jackknife	0.956	0.954	0.952	0.942	0.954

ESD = $\frac{1}{500}\sum_{r=1}^{500}\sqrt{\hat{V}\{\hat{F}(t)\}_{(r)}}$

MSE = $\frac{1}{500}\sum_{r=1}^{500}\left(\sqrt{\hat{V}\{\hat{F}(t)\}_{(r)}} - \mathrm{SD}\{\hat{F}(t)\}\right)^2$

95%Cov = Empirical coverage probability of the 95 % confidence interval

However, under $(a, b) = (0.67, 0.33)$, the Cramér–von Mises test leads to somewhat higher rejection rates than the nominal sizes. Overall, the Kolmogorov–Smirnov test produces a slightly conservative result.

Next, we examine the power under alternative hypotheses. We focus on the case of $(a, b) = (0.5, 0.5)$ under the null $F_0(t) = t\mathbb{I}(0 < t < 1)$ and alternatives

(1) $F_1(t) = t^{1/\gamma}\mathbb{I}(0 < t < 1)$, γ=1/1.8, 1/1.6, ..., 1, ..., 1.6, 1.8.
(2) $F_2(t) = t\mathbb{I}(0 < t < \gamma)/\gamma$, γ=1, 0.975, 0.95, ..., 0.75, 0.725.

As shown in Fig. 2, the power increases as γ departs from the null model of $\gamma = 1$. The curves for $\alpha = 0.05$ (right panels) are consistently higher than those for $\alpha = 0.01$ (left panels). It is found that the Cramér–von Mises test exhibits higher power than the Kolmogorov–Smirnov test under the alternative model (1). This conclusion, however, should not be overemphasized as the type I error rates of the Cramér–von Mises test

Table 5 Simulation results for the proposed goodness-of-fit tests under the null hypothesis based on 500 replications

		Cramér–von Mises test (C)			Kolmogorov–Smirnov test (K)		
		n			n		
		100	150	250	100	150	250
$(a,\ b) = (0.25, 0.75)$	Reject rate at $\alpha = 0.10$	0.096	0.097	0.100	0.075	0.075	0.095
	Reject rate at $\alpha = 0.05$	0.045	0.047	0.056	0.031	0.037	0.043
	Reject rate at $\alpha = 0.01$	0.006	0.011	0.018	0.006	0.005	0.015
	$E[C]$ or $E[K]$	0.608	0.623	0.667	0.118	0.099	0.081
	$E[C^{(b)}]$ or $E[K^{(b)}]$	0.625	0.614	0.605	0.115	0.096	0.077
$(a,\ b) = (0.5, 0.5)$	Reject rate at $\alpha = 0.10$	0.120	0.105	0.088	0.089	0.081	0.078
	Reject rate at $\alpha = 0.05$	0.063	0.055	0.045	0.037	0.033	0.030
	Reject rate at $\alpha = 0.01$	0.015	0.014	0.008	0.006	0.007	0.005
	$E[C]$ or $E[K]$	1.078	1.206	1.306	0.143	0.121	0.098
	$E[C^{(b)}]$ or $E[K^{(b)}]$	1.167	1.281	1.331	0.137	0.116	0.093
$(a,\ b) = (0.67, 0.33)$	Reject rate at $\alpha = 0.10$	0.140	0.150	0.120	0.090	0.065	0.105
	Reject rate at $\alpha = 0.05$	0.095	0.085	0.060	0.040	0.035	0.040
	Reject rate at $\alpha = 0.01$	0.015	0.020	0.030	0.010	0.005	0.010
	$E[C]$ or $E[K]$	1.006	1.109	0.989	0.142	0.118	0.091
	$E[C^{(b)}]$ or $E[K^{(b)}]$	1.001	0.984	0.820	0.135	0.113	0.087
$c = 5$	Reject rate at $\alpha = 0.10$	0.108	0.119	0.119	0.096	0.106	0.110
	Reject rate at $\alpha = 0.05$	0.063	0.057	0.059	0.052	0.055	0.055
	Reject rate at $\alpha = 0.01$	0.015	0.014	0.014	0.010	0.011	0.013
	$E[C]$ or $E[K]$	0.417	0.411	0.412	0.104	0.084	0.067
	$E[C^{(b)}]$ or $E[K^{(b)}]$	0.403	0.403	0.401	0.103	0.085	0.066

The average of the Cramér–von Mises statistics is denoted by $E[C]$. The average of its resampling version is denoted by $E[C^{(b)}]$. $E[K]$ and $E[K^{(b)}]$ are defined similarly for the Kolmogorov–Smirnov statistics

are slightly higher than those of the Kolmogorov–Smirnov test. The results for other $(a,\ b)$ are similar.

5.4 Performance of the confidence band

We investigate the coverage performance of the EP and HW bands introduced in Sect. 4.3. The EP band is calculated under p_1 =0.2 and p_2 =0.8. For each run, we check if the bands completely cover the true F. The coverage rates over the 500 replications are given in Table 6. Overall, the coverage rates reflect the nominal levels and are particularly accurate when $1 - \alpha = 0.99$. The EP band has slightly more accurate coverage compared to the HW band, especially at levels $1 - \alpha = 0.90$ and 0.95. This is because the HW band exhibits slight over-coverage, which parallels the conservative results of the Kolmogorov–Smirnov test.

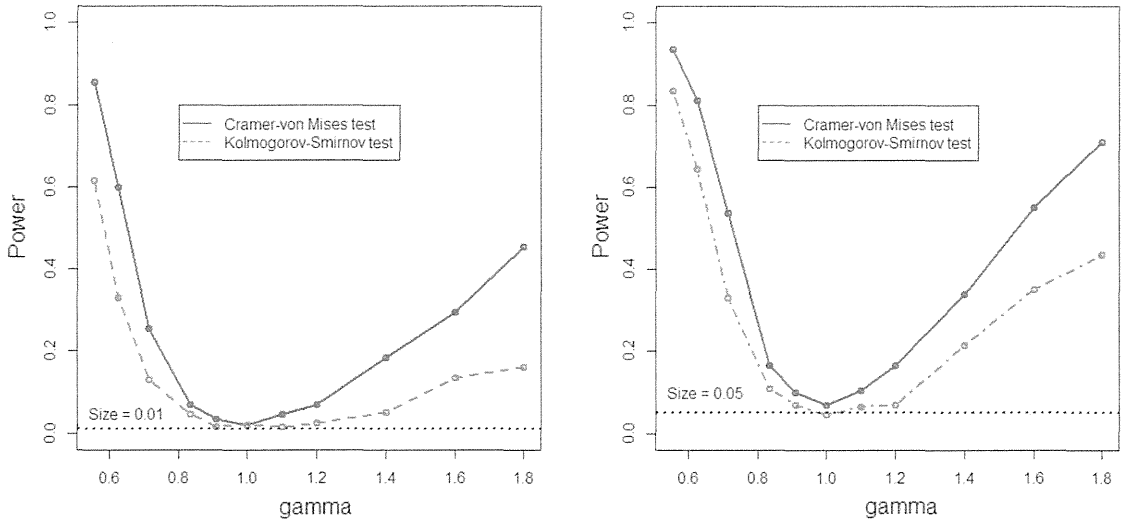

(1) Alternative $F_1(t) = t^{1/\gamma}\mathbf{I}(0 < t < 1)$, γ=1/1.8, 1/1.6, ..., 1, ..., 1.6, 1.8.

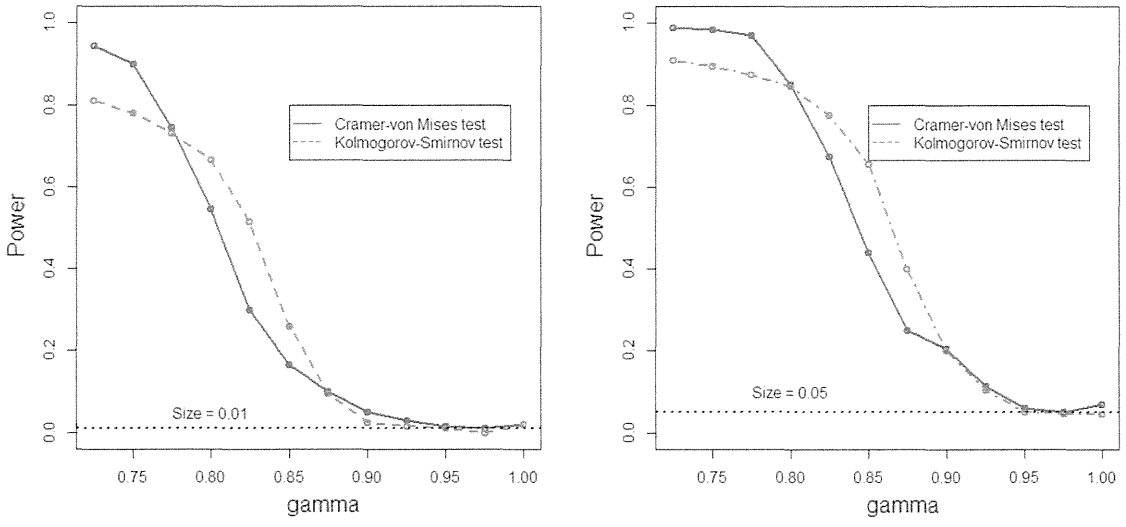

(2) Alternative $F_2(t) = t\mathbf{I}(0 < t < \gamma)/\gamma$, γ=1, 0.975, 0.95, ..., 0.75, 0.725

Fig. 2 The power curves for the proposed goodness-of-fit tests with sizes α =0.01 (*left panel*) and α =0.05 (*right panel*) based on n = 150. The value $\gamma = 1$ corresponds to the null, while $\gamma \neq 1$ corresponds to the alternative. (1) Alternative $F_1(t) = t^{1/\gamma}\mathbf{I}(0 < t < 1)$, γ=1/1.8, 1/1.6, ..., 1, ..., 1.6, 1.8. (2) Alternative $F_2(t) = t\mathbf{I}(0 < t < \gamma)/\gamma$, γ=1, 0.975, 0.95, ..., 0.75, 0.725

6 Data analysis

We analyzed the childhood cancer data from Moreira and Uña-Álvarez (2010) as described in Sect. 1. The sample consists of 409 children with $\{ (U_j, T_j, V_j) : j = 1, \ldots, 409 \}$ subject to double-truncation $U_j \leq T_j \leq V_j$, where T_j is the age (in days) at diagnosis, U_j is the age at the start of follow-up (January 1, 1999), and $V_i = U_i + 1825$ is the age at the end of follow-up (December 31, 2003). The primary interest here is inference of the distribution function $F(t) = \Pr(T^* \leq t)$, where T^* is the pre-truncated age at diagnosis. We depict the NPMLE $\hat{F}(t)$ in Fig. 3. The resulting curve is virtually identical to that reported in Moreira and Uña-Álvarez (2010). They

Table 6 Coverage rates of the proposed confidence bands at the $100(1-\alpha)\%$ level based on 500 replications

	Nominal level	$n = 100$	$n = 150$	$n = 250$
EP (equal precision) band				
$a = 0.25, b = 0.75$	$1-\alpha = 0.900$	0.904	0.924	0.902
	$1-\alpha = 0.950$	0.958	0.952	0.950
	$1-\alpha = 0.990$	0.990	0.990	0.984
$a = 0.5, b = 0.5$	$1-\alpha = 0.900$	0.908	0.910	0.918
	$1-\alpha = 0.950$	0.964	0.954	0.960
	$1-\alpha = 0.990$	0.990	0.988	0.990
$a = 0.67, b = 0.33$	$1-\alpha = 0.900$	0.915	0.905	0.910
	$1-\alpha = 0.950$	0.950	0.955	0.950
	$1-\alpha = 0.990$	0.985	0.995	0.985
$c = 5$	$1-\alpha = 0.900$	0.894	0.894	0.876
	$1-\alpha = 0.950$	0.928	0.940	0.932
	$1-\alpha = 0.990$	0.984	0.986	0.986
HW (Hall–Wellner) band				
$a = 0.25, b = 0.75$	$1-\alpha = 0.900$	0.927	0.926	0.905
	$1-\alpha = 0.950$	0.969	0.963	0.957
	$1-\alpha = 0.990$	0.994	0.995	0.985
$a = 0.5, b = 0.5$	$1-\alpha = 0.900$	0.912	0.919	0.922
	$1-\alpha = 0.950$	0.963	0.967	0.970
	$1-\alpha = 0.990$	0.994	0.993	0.995
$a = 0.67, b = 0.33$	$1-\alpha = 0.900$	0.910	0.935	0.895
	$1-\alpha = 0.950$	0.960	0.965	0.960
	$1-\alpha = 0.990$	0.990	0.995	0.990
$c = 5$	$1-\alpha = 0.900$	0.904	0.894	0.890
	$1-\alpha = 0.950$	0.948	0.945	0.945
	$1-\alpha = 0.990$	0.990	0.989	0.987

provide pointwise confidence intervals using the bootstrap. In this paper, we provide additional inference procedures using goodness-of-fit tests and confidence bands.

For goodness-of-fit tests, we set the following two hypotheses:

$$H_{01}: \quad F(t) = \frac{t}{5475}\mathbf{I}(0 < t < 5475) + \mathbf{I}(t \geq 5475)$$

and

$$H_{02}: \quad F(t) = \left(\frac{t}{5475}\right)^{3/4}\mathbf{I}(0 < t < 5475) + \mathbf{I}(t \geq 5475),$$

where $5{,}475 = 15 \times 365$ (days) is the maximum age to be defined as childhood cancer (15 years old). Here, H_{01} implies that childhood cancer occurs uniformly over all ages

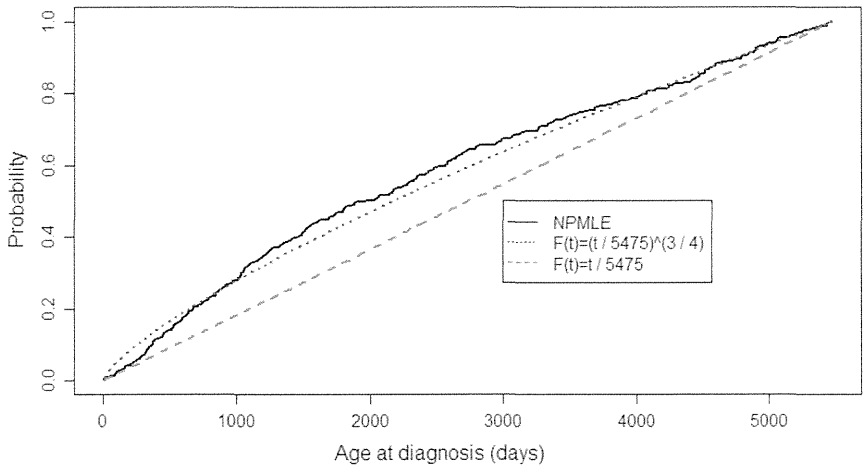

Fig. 3 The NPMLE $\hat{F}(t)$ of the distribution function of ages at diagnosis for childhood cancer (*solid line*). The hypothesized curves are $H_{01}: F(t) = (t/5475)\,\mathbb{I}(0 < t < 5475) + \mathbb{I}(t \geq 5475)$ (*dashed line*), $H_{02}: F(t) = (t/5475)^{3/4}\mathbb{I}(0 < t < 5475) + \mathbb{I}(t \geq 5475)$ (*dotted line*)

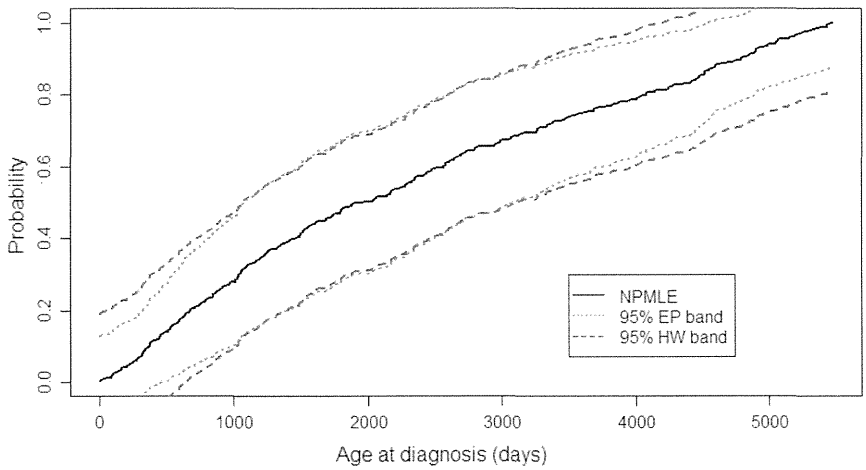

Fig. 4 The NPMLE and its 95% confidence bands. The *dotted line* is the EP (equal precision) band and the *dashed line* is the HW (Hall–Wellner) band

under 15 years, while H_{02} implies that the occurrence of childhood cancer decreases as their age increases. Figure 3 depicts the two hypothesized curves along with the NPMLE. The curve for H_{02} fits better than the curve for H_{01}. Indeed, the Cramér–von Mises test rejects H_{01} at 10 % significance level (P-value = 0.094), while does not reject H_{02} (P-value = 0.732). Similar results are found through the Kolmogorov–Smirnov test (P-value = 0.099 for H_{01} and P-value = 0.797 for H_{02}).

Figure 4 displays the 95 % EP and HW bands based on the algorithm in Sect. 4.3. The EP band is calculated under p_1 =0.1 and p_2 =0.9. The EP and HW bands are generally competitive, but the EP band is slightly narrower in the tails. This is qualitatively similar to the EP and HW bands for right-censored data. Now, we validate the coverage performance using the bootstrap as mentioned in Sect. 4.3. The EP band covers 950 out of the 1000 bootstrap NPMLEs and the HW band covers 964 out of the 1000 bootstrap NPMLEs. Hence, the coverage level is close to the nominal 95 %.

We compare the three variance estimators (proposed, bootstrap and jackknife) for selected values of t. The computation time required for the three estimators are also

Table 7 Variance estimates of the NPMLE based on the childhood cancer data

	Proposed: $\sqrt{\hat{V}_{\text{Info}}\{\hat{F}(t)\}}$	Bootstrap: $\sqrt{\hat{V}_{\text{Boot}}\{\hat{F}(t)\}}$	Jackknife: $\sqrt{\hat{V}_{\text{Jack}}\{\hat{F}(t)\}}$
Variance estimate at t = 750.0	0.0469	0.0464	0.0473
Computation time (s)	(0.25)	(342.16)	(118.37)
Variance estimate at t = 2,083.5	0.0817	0.0814	0.0815
Computation time (s)	(0.22)	(313.53)	(115.83)
Variance estimate at t = 4,251.0	0.0599	0.0665	0.0644
Computation time (s)	(0.23)	(317.48)	(117.37)

The three variance estimators are calculated at t = 750.0, t = 2,083.5, and t = 4,251.0, corresponding to the 20, 50, and 80 percentiles of observed ages at diagnosis, respectively. Required computation times for the three methods are also compared

compared. As shown in Table 7, the three estimates produce very similar results for all t. On the other hand, the computation time required for the proposed method is much shorter than those of the resampling-based methods.

7 Conclusion

This paper introduced a simple and explicit covariance estimator of the NPMLE using the observed information matrix. This technique provides various inference procedures, including pointwise confidence interval, goodness-of-fit, and confidence band.

Our simulations showed that the major advantage of the proposed variance estimator over the bootstrap and jackknife was for the larger samples (n = 250 and 300). The data analysis demonstrated the reduced computational time for the proposed method vis-à-vis the bootstrap and jackknife methods. Hence, the proposed method is most useful when the sample size is very large, which often occurs in demography and epidemiology (e.g., Stovring and Wang 2007). In such large-scale studies, the proposed method may be the best possible choice for statistical inference.

For goodness-of-fit procedures, we developed the Kolmogorov–Smirnov and Cramér–von Mises tests with the null distributions simulated by the proposed covariance structure. The simulations showed that these tests have proper type I error rates and power. Applying the tests to the childhood cancer data, we rejected the scientific assumption that childhood cancer occurs uniformly over all ages below 15 years. This conclusion could not have been derived without developing the goodness-of-fit procedures.

Acknowledgments We would like to thank the editor, the associate editor and the two reviewers for their helpful comments and corrections that greatly improved the manuscript. This work was financially supported by the National Science Council of Taiwan (NSC101-2118-M008-002-MY2) to T. Emura, and a Grant-in-Aid for a Research Fellow of the Japan Society for the Promotion of Science to H. Michimae (No. 23570036). The work of Y. Konno was partially supported by Grant-in-Aid for Scientific Research(C) (No. 25330043 and 21500283).

Appendix A: Bootstrap and jackknife algorithms

Simple bootstrap algorithm (Moreira and Uña-Álvarez 2010):

Step 1: For each $b = 1, \ldots, B$, draw bootstrap resamples $\{ (U_{jb}^*, T_{jb}^*, V_{jb}^*) : j = 1, \ldots, n \}$ from $\{ (U_j, T_j, V_j) : j = 1, \ldots, n \}$, and then compute the NPMLE $\hat{F}_b^*(t)$ from them.
Step 2: Compute the bootstrap variance estimator

$$\hat{V}_{\text{Boot}}\{\hat{F}(t)\} = \frac{1}{B-1}\sum_{b=1}^{B}\{\hat{F}_b^*(t) - \bar{F}^*(t)\}^2,$$

where $\bar{F}^*(t) = \frac{1}{B}\sum_{b=1}^{B}\hat{F}_b^*(t)$, and take the $(\alpha/2)\times 100\%$ and $(1-\alpha/2)\times 100\%$ points of $\{ \hat{F}_b^*(t) : b = 1, \ldots, B \}$ for the$(1-\alpha)\times 100\%$ confidence interval.

Jackknife algorithm:

Step 1: For each $i = 1, \ldots, n$, delete the i th sample from $\{ (U_j, T_j, V_j) : j = 1, \ldots, n \}$, and then compute the NPMLE $\hat{F}_{(-i)}(t)$ from the remaining $n-1$ samples.
Step 2: Compute the jackknife variance estimator

$$\hat{V}_{\text{Jack}}\{\hat{F}(t)\} = \frac{n-1}{n}\sum_{i=1}^{n}\{\hat{F}_{(-i)}(t) - \bar{F}_{(\cdot)}(t)\}^2,$$

where $\bar{F}_{(\cdot)}(t) = \frac{1}{n}\sum_{i=1}^{n}\hat{F}_{(-i)}(t)$, and the log-transformed $(1-\alpha)\times 100\%$ confidence interval

$$\left(\hat{F}(t)\exp[\, -z_{\alpha/2}\hat{V}_{\text{Jack}}^{1/2}\{\hat{F}(t)\}/\hat{F}(t)\,],\quad \hat{F}(t)\exp[\, z_{\alpha/2}\hat{V}_{\text{Jack}}^{1/2}\{\hat{F}(t)\}/\hat{F}(t)\,] \right).$$

Appendix B: Asymptotic theory

Appendix B1. Weak convergence of $\sqrt{n}(\,\hat{F}(t) - F(t)\,)$

Although not stated explicitly, we assume that the identifiability conditions (Shen 2010, p. 836) are satisfied. Consider the log-likelihood function

$$\ell_n(F)/n = \sum_{i=1}^{n}(\log f_j - \log F_j)/n.$$

For any $h \in Q$, where Q is the set of all uniformly bounded functions, let $H(t) = \int_0^t h(s)dF(s)$ and $\hat{H}(t) = \int_0^t h(s)d\hat{F}(s)$ where h satisfies the constraint $\hat{H}(\infty) = 1$. Suppose that $\hat{F}$ is the maximizer of $\ell_n(F)$. Then for any $h \in Q$ and $\varepsilon \geq 0$, we have $\ell_n(\hat{F} + \varepsilon\hat{H}) \leq \ell_n(\hat{F})$. Hence, the score function $\partial\ell_n(F + \varepsilon H)/\partial\varepsilon|_{\varepsilon=0}$ is equal to

$$\Psi_n(F)[h] \equiv \frac{1}{n}\sum_{i=1}^{n}\left[h(T_i) - \frac{\int \mathbb{I}(U_i \le s \le V_i)h(s)dF(s)}{\int \mathbb{I}(U_i \le s \le V_i)dF(s)}\right],$$

for any $h \in Q$. The expectation is defined as

$$\Psi(F)[h] \equiv E\left[h(T^*) - \frac{\int \mathbb{I}(U^* \le s \le V^*)h(s)dF(s)}{\int \mathbb{I}(U^* \le s \le V^*)dF(s)}\right].$$

Consider $\Psi_n(F)[h]$ as a random function defined on Q. Accordingly, consider a random map $\Theta \to l^\infty(Q)$, defined by $F \mapsto \Psi_n(F)[\cdot]$. Then, the equation $\Psi_n(F)[\cdot] = 0$ is considered the estimating function that takes its value on $l^\infty(Q)$. It follows that the NPMLE is the Z-estimator that satisfies $\Psi_n(\hat{F})[\cdot] = 0$ (van der Vaart and Wellner 1996, p. 309). In the following, we assume that certain regularity conditions for the asymptotic theory for the Z-estimator hold, which include the asymptotic approximation condition, the Fréchet differentiability of the map, and the invertibility of the derivative map.

Then, one can write

$$0 = n^{1/2}\Psi_n(\hat{F})[h] = n^{1/2}\Psi_n(F)[h] + n^{1/2}\dot{\Psi}_F(\hat{F} - F)[h] + o_P(1), \tag{5}$$

where $\dot{\Psi}_F(\hat{F} - F)[h]$ is the derivative of $\Psi_n(F)[h]$ at F with direction $\hat{F} - F$. It follows from the form of $\Psi(F)[\cdot]$ that

$$\dot{\Psi}_F(\hat{F} - F)[h] = \frac{d}{dt}\Psi\{\ \hat{F} + t(\hat{F} - F)\ \}[h]|_{t=0} = -\int \sigma_F(x)[h]d(\hat{F} - F)(x). \tag{6}$$

It follows from Eqs. (5) and (6) that the NPMLE satisfies the asymptotic linear expression

$$\begin{aligned}&\sqrt{n}\int \sigma_F(x)[h]d(\hat{F} - F)(x)\\ &= \frac{1}{\sqrt{n}}\sum_{i=1}^{n}\left[h(T_i) - \frac{\int I(U_i \le s \le V_i)h(s)dF(s)}{\int I(U_i \le s \le V_i)dF(s)}\right] + o_P(1),\end{aligned} \tag{7}$$

where the right-side converges weakly to a mean zero Gaussian process with the covariance structure

$$\begin{aligned}&E\left[h(T^*) - \frac{\int \mathbb{I}(U^* \le s \le V^*)h(s)dF(s)}{\int \mathbb{I}(U^* \le s \le V^*)dF(s)}\right]\left[h'(T^*) - \frac{\int \mathbb{I}(U^* \le s \le V^*)h'(s)dF(s)}{\int \mathbb{I}(U^* \le s \le V^*)dF(s)}\right]\\ &= \int \sigma_F(x)[h]h'(x)dF(x),\end{aligned}$$

for bounded functions h and h'. The desired weak convergence of $\sqrt{n}(\ \hat{F}(t) - F(t)\ )$ is obtained by setting $h = \sigma_F^{-1}(w_t)$ in Eq. (7).

Appendix B2: Proof of $\sum_{j=1}^{n} w_s(T_j)\hat{\sigma}_F^{-1}(w_t)(T_j)\hat{f}_j = \mathbf{W}_s^{\mathrm{T}} \left\{ \frac{i_n(\mathbf{f})}{n} \right\}^{-1} \mathbf{W}_t$

It follows that

$$\hat{\sigma}_F(T_j)[h] = \frac{1}{n}\sum_{i=1}^{n} J_{ij}\left\{ \frac{h_j}{\hat{F}_i} - \frac{1}{\hat{F}_i^2}\sum_{k=1}^{n} J_{ik}h_k\hat{f}_k \right\} = \frac{1}{n}\left[\frac{h_j\hat{f}_j}{\hat{f}_j^2} - \sum_{i=1}^{n}\sum_{k=1}^{n} \frac{J_{ij}J_{ik}}{\hat{F}_i^2} h_k\hat{f}_k \right]. \tag{8}$$

Note that

$$J^{\mathrm{T}}\mathrm{diag}\left(\frac{1}{\mathbb{F}^2}\right) J = \begin{bmatrix} \sum_{i=1}^{n} \frac{J_{i1}J_{i1}}{F_i^2} & \cdots & \sum_{i=1}^{n} \frac{J_{i1}J_{in}}{F_i^2} \\ \vdots & \ddots & \vdots \\ \sum_{i=1}^{n} \frac{J_{in}J_{i1}}{F_i^2} & \cdots & \sum_{i=1}^{n} \frac{J_{in}J_{in}}{F_i^2} \end{bmatrix}.$$

Hence, Eq. (8) with $h = h'$ and $\sigma_F(x)[h'] = w_t(x) = \mathbb{I}(x \le t)$ yield

$$\begin{aligned} \begin{bmatrix} w_t(T_1) \\ \vdots \\ w_t(T_n) \end{bmatrix} &= \frac{1}{n}\left[\left\{ \mathrm{diag}\left(\frac{1}{\hat{\mathbf{f}}^2}\right) - J^{\mathrm{T}}\mathrm{diag}\left(\frac{1}{\hat{\mathbb{F}}^2}\right) J \right\}\Big|_{\hat{f}_n = 1 - \mathbf{1}_{n-1}^{\mathrm{T}}\hat{\mathbf{f}}} \right] \begin{bmatrix} h_1\hat{f}_1 \\ \vdots \\ h_n\hat{f}_n \end{bmatrix} \\ &= \frac{1}{n}\left[\left\{ \mathrm{diag}\left(\frac{1}{\hat{\mathbf{f}}^2}\right) - J^{\mathrm{T}}\mathrm{diag}\left(\frac{1}{\hat{\mathbb{F}}^2}\right) J \right\}\Big|_{\hat{f}_n = 1 - \mathbf{1}_{n-1}^{\mathrm{T}}\hat{\mathbf{f}}} \right] D^{\mathrm{T}} \begin{bmatrix} h_1\hat{f}_1 \\ \vdots \\ h_{n-1}\hat{f}_{n-1} \end{bmatrix}, \end{aligned}$$

where the last equation uses the constraint $\sum_{j=1}^{n} h_j\hat{f}_j = 0$. Multiplying D for both sides, and taking the inverse of the information matrix,

$$\begin{bmatrix} \hat{\sigma}_F^{-1}(w_t)(T_1)\hat{f}_1 \\ \vdots \\ \hat{\sigma}_F^{-1}(w_t)(T_{n-1})\hat{f}_{n-1} \end{bmatrix} = \left\{ \frac{i_n(\hat{\mathbf{f}})}{n} \right\}^{-1} \begin{bmatrix} w_t(T_1) - w_t(T_n) \\ \vdots \\ w_t(T_1) - w_t(T_n) \end{bmatrix}.$$

It follows that

$$\begin{aligned} \sum_{j=1}^{n} w_s(T_j)\hat{\sigma}_F^{-1}(w_t)(T_j)\hat{f}_j &= \sum_{j=1}^{n-1} \{\, w_s(T_j) - w_s(T_n) \,\}\hat{\sigma}_F^{-1}(w_t)(T_j)\hat{f}_j \\ &= \left[\, w_s(T_1) - w_s(T_n) \cdots w_s(T_{n-1}) - w_s(T_n) \,\right] \left\{ \frac{i_n(\hat{\mathbf{f}})}{n} \right\}^{-1} \begin{bmatrix} w_t(T_1) - w_t(T_n) \\ \vdots \\ w_t(T_1) - w_t(T_n) \end{bmatrix} \\ &= \mathbf{W}_s^{\mathrm{T}} \left\{ \frac{i_n(\hat{\mathbf{f}})}{n} \right\}^{-1} \mathbf{W}_t. \end{aligned}$$

References

Austin D, Simon DK, Betensky RA (2013) Computationally simple estimation and improved efficiency for special cases of double truncation. Lifetime Data Anal. doi:10.1007/s10985-013-9287-z

Chen YH (2010) Semiparametric marginal regression analysis for dependent competing risks under an assumed copula. J R Stat Soc B 72:235–251

Commenges D (2002) Inference for multi-state models from interval-censored data. Stat Methods Med Res 11:167–182

Efron B, Petrosian V (1999) Nonparametric method for doubly truncated data. J Am Stat Assoc 94:824–834

Emura T, Wang W (2012) Nonparametric maximum likelihood estimation for dependent truncation data based on copulas. J Multivar Anal 110:171–188

Emura T, Konno Y (2012) Multivariate normal distribution approaches for dependently truncated data. Stat Papers 53:133–149

Klein JP, Moeschberger ML (2003) Survival analysis: techniques for censored and truncated data. Springer, New York

Moreira C, Uña-Álvarez J (2010) Bootstrapping the NPMLE for doubly truncated data. J Nonparametr Stat 22:567–583

Moreira C, Uña-Álvarez J (2012) Kernel density estimation with doubly-truncated data. Electron J Stat 6:501–521

Moreira C, Keilegom IV (2013) Bandwidth selection for kernel density estimation with doubly truncated data. Comput Stat Data Anal 61:107–123

Moreira C, Uña-Álvarez J, Meira-Machado L (2014) Nonparametric regression with doubly truncated data. Comput Stat Data Anal. doi:10.1016/j.csda.2014.03.017

Murphy SA (1995) Asymptotic theory for the frailty model. Ann Stat 23:182–198

Nair VN (1984) Confidence bands for survival functions with censored data: a comparative study. Technometrics 26:265–275

Shen PS (2010) Nonparametric analysis of doubly truncated data. Ann Inst Stat Math 62:835–853

Shen PS (2011) Testing quasi-independence for doubly truncated data. J Nonparametr Stat 23:1–9

Shen PS (2012) Empirical likelihood ratio with doubly truncated data. J Appl Stat 38:2345–2353

Stovring H, Wang MC (2007) A new approach of nonparametric estimation of incidence and lifetime risk based on birth rates and incidence events. BMC Med Res Methodol 7:53

van der Vaart AW, Wellner JA (1996) Weak convergence and empirical process. Springer-Varlag, New York

Zeng D, Lin DY (2006) Efficient estimation of semiparametric transformation models for counting processes. Biometrika 93:627–640

Zhu H, Wang MC (2012) Analyzing bivariate survival data with interval sampling and application to cancer epidemiology. Biometrika 99:345–361

Cancer Chemother Pharmacol (2014) 73:895–901
DOI 10.1007/s00280-014-2418-8

ORIGINAL ARTICLE

A phase I study of irinotecan and pegylated liposomal doxorubicin in recurrent ovarian cancer (Tohoku Gynecologic Cancer Unit 104 study)

Tadahiro Shoji · Eriko Takatori · Yoshitaka Kaido · Hideo Omi · Yoshihito Yokoyama · Hideki Mizunuma · Michiko Kaiho · Takeo Otsuki · Tadao Takano · Nobuo Yaegashi · Hiroshi Nishiyama · Keiya Fujimori · Toru Sugiyama

Received: 24 October 2013 / Accepted: 14 February 2014 / Published online: 1 March 2014

Abstract
Purpose A phase I clinical study was conducted to determine the maximum tolerated dose (MTD) and the recommended dose (RD) of irinotecan hydrochloride (CPT-11) in CPT-11/pegylated liposomal doxorubicin (PLD) combination therapy, a novel treatment regimen for platinum- and taxane-resistant recurrent ovarian cancer.
Methods Pegylated liposomal doxorubicin was administered intravenously on day 3 at a fixed dose of 30 mg/m^2. CPT-11 was administered intravenously on days 1 and 15, at a dose of 50 mg/m^2 on both days. One course of chemotherapy was 28 days, and patients were given a maximum of six courses, with the CPT-11 dose being increased in increments of 10 mg/m^2 (level 1, 50 mg/m^2; level 2, 60 mg/m^2; level 3, 70 mg/m^2; level 4, 80 mg/m^2) to determine MTD and RD.
Results During the period from April 2010 to March 2013, three patients were enrolled for each level. In the first course, no dose-limiting toxicity occurred in any of the patients. Grade 4 neutropenia was observed in two of three patients at level 4. At level 4, the antitumor effect was a partial response (PR) in two of the three patients and stable disease (SD) in one. At level 3, one of the three patients showed PR and two had SD. At level 4, the start of the next course was postponed in two of three patients. In addition, one patient at level 4 experienced hemotoxicity that met the criteria for dose reduction in the next course. The above results suggested that administration of CPT-11 at dose level 5 (90 mg/m^2) would result in more patients with severe neutropenia and in more patients requiring postponement of the next course or a dose reduction. Based on the above, the RD of CPT-11 was determined to be 80 mg/m^2.
Conclusions The results suggest that CPT-11/PLD combination therapy for recurrent ovarian cancer is a useful treatment method with a high response rate and manageable adverse reactions. In the future phase II study, the safety and efficacy of this therapy will be assessed at 80 mg/m^2 of CPT-11 and 30 mg/m^2 of PLD.

Keywords Recurrent ovarian cancer · Chemotherapy · CPT-11 · PLD

T. Shoji (✉) · E. Takatori · Y. Kaido · H. Omi · T. Sugiyama
Department of Obstetrics and Gynecology, Iwate Medical University School of Medicine, 19-1 Uchimaru, Morioka 020-8505, Japan
e-mail: tshoji@iwate-med.ac.jp

Y. Yokoyama · H. Mizunuma
Department of Obstetrics and Gynecology, Hirosaki University School of Medicine, 53 Honcho, Hirosaki 036-8563, Japan

M. Kaiho · T. Otsuki · T. Takano · N. Yaegashi
Department of Obstetrics and Gynecology, Tohoku University Graduate School of Medicine, 1-1 Seiryouchou, Sendai 980-8574, Japan

H. Nishiyama · K. Fujimori
Department of Obstetrics and Gynecology, Fukushima Medical University School of Medicine, 1 Hikarigaoka, Fukushima 960-1295, Japan

Introduction

The standard initial chemotherapy for advanced ovarian cancer is paclitaxel plus carboplatin (TC) combination therapy [1–3]. However, no treatment regimen for second-line chemotherapy has yet been established against recurrence after TC therapy. Various attempts are currently being made using, as criteria, the type of recurrence and the period from the last treatment until recurrence. Since recurrent

ovarian cancer with a treatment-free interval (the period from the end of the initial chemotherapy until recurrence) of <6 months is considered to be platinum resistant, it will be essential to select drugs not showing cross-resistance with the initial therapy. In the United States and Europe, the type I DNA topoisomerase inhibitor topotecan [4], pegylated liposomal doxorubicin (PLD) [5], and gemcitabine [6] are used against platinum-resistant recurrent ovarian cancer. In a Japanese phase II study involving patients with ovarian cancer previously treated with chemotherapy including platinum-based agents, PLD was reported to achieve an overall response rate of 21.9 % (27.3 % [3/11] in the platinum-sensitive group and 21.0 % [13/62] in the platinum-resistant group) [7]. In a phase III non-inferiority study comparing PLD with topotecan, it was reported that in patients treated with PLD, the response rate was 19.7 %, median progression-free survival (PFS) was 16.1 weeks, and mean survival time (MST) was 60.0 weeks and, in patients with platinum-resistant tumors in particular, the response rate was 12.3 %, median PFS was 9.1 weeks, and MST was 35.6 weeks [8], suggesting that PLD would be a promising therapeutic agent for recurrent ovarian cancer. On the other hand, irinotecan hydrochloride (CPT-11), an anticancer agent developed in Japan, acts by inhibiting topoisomerase I. In a study in which CPT-11 (100 mg/m^2) alone was administered to patients with platinum-resistant recurrent ovarian cancer, the response rate was 29 %, the tumor growth inhibition rate (complete response [CR] + partial response [PR] + not changed) was 61 %, median time to progression was 17 weeks, and MST was 8 months, exhibiting favorable results [9]. Sugiyama et al. [10] reported that CPT-11/cisplatin therapy was effective as second-line chemotherapy for recurrent ovarian cancer after treatment with a platinum agent, raising the expectation that CPT-11 may be effective against platinum- and taxane-resistant tumors.

Herein, we conducted a phase I clinical study to determine the maximum tolerated dose (MTD) and the recommended dose (RD) of CPT-11 in CPT-11/PLD combination therapy, a novel treatment regimen for platinum- and taxane-resistant recurrent ovarian cancer, with the aim of improving the outcomes of ovarian cancer patients.

Subjects and methods

Study population

Upon receiving approval from the intramural ethics committee of each study center, a multicenter clinical study was conducted in patients with recurrent ovarian cancer who met the following criteria and were enrolled in the study during the period from April 2010 to March 2013: (1) ovarian cancer confirmed by histological or cytological diagnosis, (2) recurrence less than 6 months after previous chemotherapy, (3) containing a measurable or evaluable lesion (including CA-125 level), (4) ECOG performance status (PS) 0–2, (5) 20–75-year old, (6) expected survival time of at least 2 months, (7) major organs remained functional (white blood cell count $\geq$3,000/mm^3, neutrophil count $\geq$1,500/mm^3, platelet count $\geq$10,0000/mm^3, total bilirubin $\leq$1.5 mg/dL), and (8) informed consent provided. Exclusion criteria were (1) serious complication(s), (2) evident pulmonary fibrosis or interstitial pneumonitis, (3) pleural or cardiac effusion necessitating prompt local treatment, (4) brain metastasis requiring prompt treatment, (5) diarrhea (watery stool), (6) intestinal paralysis or intestinal obstruction, (7) active infection requiring treatment with antimicrobial agents, and (8) patients considered inappropriate as subjects by the physician in charge for any other reason.

Protocol

Pegylated liposomal doxorubicin was administered intravenously at a fixed dose of 30 mg/m^2 on day 3. CPT-11 was administered intravenously on days 1 and 15. One course of chemotherapy was 28 days, and as a general rule, patients were given at least 2 courses, 6 courses at the maximum.

Method for dose escalation

CPT-11 was started at level 1 (50 mg/m^2) and then increased up to level 4 (80 mg/m^2) (Table 1). A group of three patients were given the same dose level of CPT-11, and if no dose-limiting toxicity (DLT) was observed in any of them, the dose was increased to the next level. If DLT was observed in one of the three patients at the same level, three additional patients were treated at the same dose level, and if there was no observable DLT in at least three of the total six patients, the dose was increased to the next level. If DLT was observed in at least three of the total six patients, the dose was judged to be MTD. If DLT was observed in two of three patients at any level, this dose level was judged to be MTD. The dose that was 1 level below MTD was determined to be RD. DLT was defined as (1) grade

Table 1 Dose escalation schema

	CPT-11 (mg/m^2)	PLD (mg/m^2)
Level 0	40	30
Level 1	50	30
Level 2	60	30
Level 3	70	30
Level 4	80	30

4 leukopenia or neutropenia lasting for at least 4 days, (2) grade 3 or higher leukopenia or neutropenia accompanied by pyrexia of ≥38 °C, (3) grade 4 or higher thrombocytopenia or thrombocytopenia requiring platelet transfusion, or (4) grade 3 or higher nonhematological toxicity (except nausea/vomiting, anorexia, and general malaise). Adverse events were evaluated according to NCI-CTCAE ver. 3, and MTD was determined during the first course.

Criteria for changing dosing schedule

If any of the following applied, CPT-11 administration on day 15 was to be postponed and the drug was to be administered on day 22 upon confirming recovery from the condition: (1) white blood cell count ≤2,000/mm^3, (2) neutrophil count ≤1,000/mm^3, (3) platelet count ≤75,000/mm^3, or (4) grade 1 or higher diarrhea. If recovery from the condition was not seen on day 22, the second CPT-11 administration was to be skipped (not to be administered on day 29). The criteria for proceeding to the second and subsequent courses were (1) white blood cell count ≥3,000/mm^3, (2) neutrophil count ≥1,500/mm^3, (3) platelet count ≥100,000/mm^3, (4) total bilirubin ≤1.5 mg/dL, (5) diarrhea grade 0, and (6) grade 1 or lower hand-and-foot syndrome and stomatitis. If the patient met any of the above criteria, administration was to be performed after waiting for recovery for a maximum of 14 days. If recovery from these conditions was not seen after 14 days, the treatment was to be discontinued. If the severity of hand-and-foot syndrome or stomatitis remained at grade 2 or higher after a 14-day postponement, PLD on day 3 in the next course was to be skipped.

Criteria for dose reduction

The doses of CPT-11 and PLD in the next course were reduced according to the severity of adverse reactions that occurred in the previous course. If grade 4 leukopenia, grade 4 neutropenia, or grade 3 thrombocytopenia were observed in the previous course, CPT-11 was reduced by 10 mg/m^2, and PLD by 7.5 mg/m^2. If grade 2 or higher diarrhea, spasmodic abdominal pain, or watery stool were observed, the CPT-11 dose was reduced by 10 mg/m^2. If grade 3 hand-and-foot syndrome or stomatitis was observed, the PLD dose was reduced by 7.5 mg/m^2 regardless of whether or not these conditions improved before the start of the next course.

Evaluation of antitumor effect

The antitumor effect was evaluated by imaging at the end of every two courses. For the evaluation of the antitumor effect, the best response rate was calculated according to the Response Evaluation Criteria in Solid Tumors (RECIST) guideline.

Results

Patient background characteristics

Table 2 shows the background characteristics of 12 patients enrolled in this study during the period from April 2010 through March 2013. All patients had been treated with taxane- or platinum-based agents as a part of the previous therapy.

Adverse events

Three patients were enrolled for each level, and none of them experienced DLT in the first course. No grade 3 or higher neutropenia was observed at level 1. Grade 4 leukopenia was observed in one patient each at level 2 and level 3, and in two patients at level 4. No grade 3 or higher thrombocytopenia was observed at level 1 or 2. At level 3, grade 3 thrombocytopenia was observed in one patient, and at level 4, two patients developed grade 2 thrombocytopenia, while no grade 3 or higher thrombocytopenia

Table 2 Patients characteristics (N=12)

Age	
Median	56
Range	40–65
PS	
0	11
1	1
FIOG stage	
I	2
II	1
III	8
IV	1
Histological type	
Serous	8
Mucinus	0
Clear cell	3
Endometrioid	1
Previous regimens	
1	4
2	3
3≤	5
Last regimen	
TC	8
TP	1
DP	1
CDDP/VP16	1
PTX	1

TC paclitaxel/carboplatin, *TP* paclitaxel/cisplatin, *DP* docetaxel/cisplatin, *CDDP* cisplatin, *PTX* paclitaxel